The 2009 IEEE/RSJ International Conference on
Intelligent Robots and Systems
October 11-15, 2009 St. Louis, USA

Semi-autonomous Operation of Tracked Vehicles on Rough Terrain using Autonomous Control of Active Flippers

Yoshito Okada, Keiji Nagatani and Kazuya Yoshida

Abstract— **For tracked vehicles moving over rough terrain, it is important to avoid rollovers and rapid motion. To realize smooth locomotion on rough terrain, some tracked vehicles are equipped with "active flippers." Such flippers increase the traversability and stability of tracked vehicles. However, their control increases the operator workload, especially in the case of teleoperation.**

To eliminate this problem, we have developed an autonomous controller for generating terrain-reflective motions of flippers. Terrain information is obtained using laser range sensors that are located at both sides of our tracked vehicle testbed. Using this system, operators only have to specify a direction to the robot, following which the robot traverses rough terrain using autonomous flipper motions. In this paper, we introduce a strategy and an algorithm for the controller for active flippers and validate the reliability of the system through experimental results on rough terrain.

I. INTRODUCTION

In areas affected by natural or man-made disasters, a trade-off exists between conducting search and rescue operations to save victims of the primary disaster and minimizing the risk of secondary disasters to rescuers and victims in the area. The risk to human life can be minimized by using robotic technology for such operations; therefore, the demand for such technology has increased significantly in recent years [1].

To operate effectively in such hazardous environments, mobile search and rescue robots should have high mobility on rough terrain. Tracked vehicles are frequently used as rescue robots since they satisfy this requirement. Our group has been developing tracked vehicles for the purpose of search and rescue operations.

In this study, we performed experiments using "Kenaf," a tracked vehicle testbed equipped with four active flippers (Fig. 1). The experiments involved climbing up/down a flight of stairs and traversing rough terrain; in addition, we entered Kenaf in the Robocup Rescue League [2]. Through such experiments and competitions, we observed that the use of flippers improves traversability on rough terrain significantly. However, it also increases the workload of operators controlling the robots, particularly in a situation where the vehicle and the operator may be far apart and the environment around the robot is unknown, like the case in the Robocup Rescue League.

This work was supported by Strategic Advanced Robot Technology, an R&D project of the NEDO, Japan.

Y.Okada, K.Nagatani and K.Yoshida are with Tohoku University, 6-6-01 Aramaki Aza Aoba, Aoba-ku, Sendai 980-8579, JAPAN, yoshito@astro.mech.tohoku.ac.jp

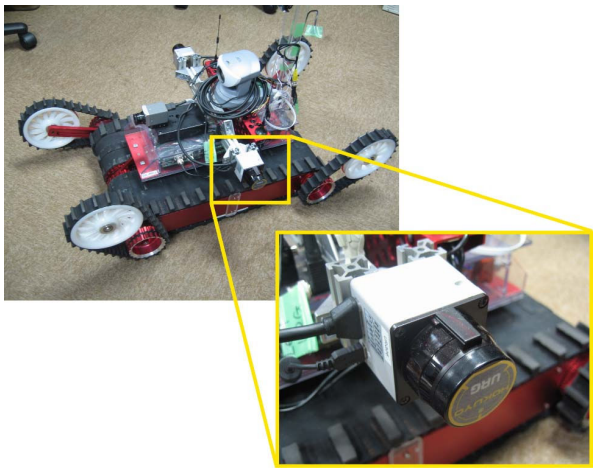

Fig. 1. Tracked vehicle testbed Kenaf equipped with laser range sensors

TABLE I
BASIC SPECIFICATIONS OF KENAF

Dimensions	W400 [mm] × L500 [mm]
Weight	20 [kg]
Length of flippers	235 [mm]
Degrees of freedom	6 (2 main tracks and 4 flippers)

To reduce the operator workload, we proposed a terrain-reflective autonomous controller for flippers that enables tracked vehicles to operate semi-autonomously [3]. Realtime terrain and posture information is obtained using two laser range sensors attached at both sides of Kenaf, and 3 D.O.F. gyroscopes and gravity sensors, respectively [4]. Using the obtained sensor information, the flipper angles are controlled to negotiate the terrain and move over bumps or steps. This method was successfully implemented on Kenaf, and it was found to reduce the operator workload considerably. However, operational tests in various environments revealed that our system had a few limitations. Therefore, in this study, we aim to improve upon our previous controller and develop a new autonomous controller for flippers.

There have been several studies on tracked vehicles having active/passive flippers for traversing rough terrain [5][6]. ROBHAZ-DT3 [5] has a main track divided into anterior and posterior tracks that are linked passively. The anterior track has triangular sides. This robot is designed to traverse steps and stairs using passive motions of the link by transiting the triangular sides of the anterior track making contact with such kind of terrains.

A controller for the active motion of a flipper has also been

reported; this controller judges whether the robot contacts the ground using current sensors that measure torque of each flipper and PSD sensors that are located at the front and back of the robot body [6]. The velocity of each flipper is determined based on the abovementioned judgment and the posture of the robot. This controller is quite simple and small; however, it cannot generate terrain-reflective motions of flippers because the PSD sensors have a limited detection range.

For traversing rough, complex, and unknown terrain, an autonomous controller for active flippers that can generate terrain-reflective motions appears to be more effective than a sensor-reflective controller or a passive mechanism. Therefore, we employ an autonomous controlled to realize semi-autonomous operation for rescue robots.

This paper is organized as follows. In Sec. II, we introduce our strategy for the autonomous control of flippers; this strategy is based on the motions of flippers teleoperated by expert operators. In Sec. III, we present a detailed description of an algorithm for realizing the strategy described in Sec. II. Then, we applied the proposed controller to Kenaf and performed actual experiments in simulated disaster environments to confirm its validity. In Sec. IV, we report the results of our experiments and present the discussions. Finally, we present the conclusions of our study in Sec. V.

II. Strategy for Controller for Flippers

A previous study [3] revealed three limitations of our previous controller. First, although terrain information along the entire length of both sides of Kenaf could be obtained using the two laser range sensors, only a part of the terrain information around the front flippers was used. In other words, the reference positions of the front flippers were determined using partial terrain information while those of the rear flippers were determined without using any terrain information. Second, the front reference positions were determined by an approximate geometric method on the assumption that the flippers are rod-shaped, although their actual shape is more complex. Finally, the previous controller could not perform realtime stability analysis. Although we have discussed stability analysis in our previous study, we did not implement our findings in the previous controller. In fact, the analysis was only used to check whether a rescue operation could be continued.

Considering these limitations, we devised a new strategy for an autonomous controller for flippers that was based on the motions of flippers teleoperated by expert operators. From the expert operators, we observed the following.

- To enable the robot to traverse terrain smoothly, its posture must be maintained according to the slope of the ground surface.
- To enable good locomotion, the main tracks and flippers should make contact with the ground to the greatest extent possible.
- When the pose of the robot is unstable, its rollover should be prevented by the motion of the flippers.

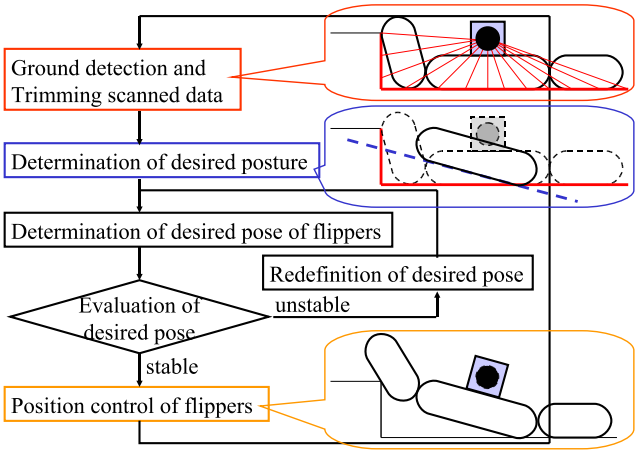

Fig. 2. Algorithm for autonomous controller for flippers

Considering the above three points, we devised a new control strategy for the flippers and the robot body as follows:

- The posture of the robot body must be maintained parallel to the least-squares plane of the ground surface and the robot body must make contact with the ground.
- The desired posture can be realized by changing the positions of the flippers.
- The desired pose (desired posture and flipper positions) must be evaluated and redefined if it is unstable.

Fig. 2 shows the new algorithm for an autonomous controller for flippers that is based on the above strategy that eliminates the disadvantages of the previous one. This algorithm is summarized as given below.

(1) The ground surface along both sides of the vehicle is first detected using the laser range sensors, and a target area of the detected surface is determined. Then, (2) the desired posture of the body is calculated based on the least-squares plane of the surface. Using the desired posture, (3) the desired positions of the flippers are also determined by a rigorous geometric calculation. Next, (4) a stability criterion is calculated. If the stability criterion does not exceed a threshold value, (5) the desired pose is redefined, and steps (3)-(5) are repeated.

The above procedure is described in detail in the following section.

III. Algorithm for Controller for Flippers

A. Ground detection and trimming scanned data

The ground surface is translated into range data of measured points by the two laser range sensors. Considering the time delay until the desired pose is realized, the target measured points would be those that would be under the robot if it were to take the desired pose. Therefore, we trim away some of n measured points $V = \{v_1, ..., v_n\}$ if a point does not satisfy the following requirement:

$$-L_{max}/2 \leqq x_{v_i} - V_r \cdot \Delta t \leqq L_{max}/2 (i = 1, ..., n) \quad (1)$$

where L_{max} is the maximum length of Kenaf including the flippers; Δt, the estimated time delay for swinging the

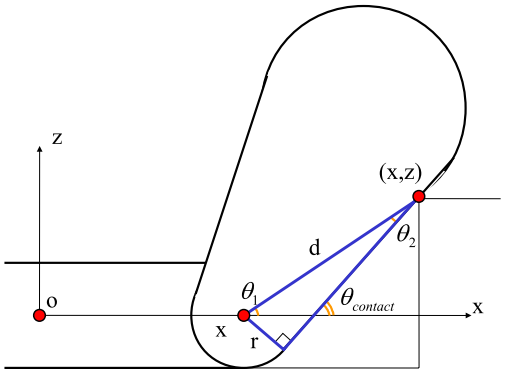

Fig. 3. Contact angle of the straight section of the flipper

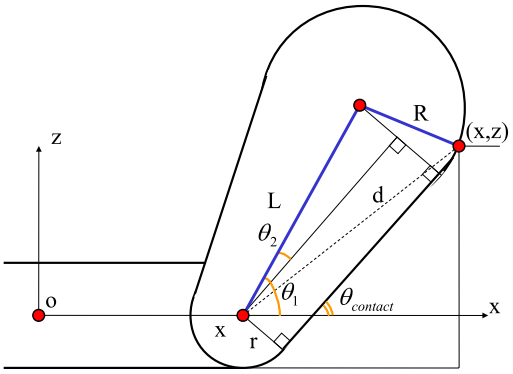

Fig. 4. Contact angle of the round section of the flipper

flippers; and V_r, the velocity of the robot. In addition, the measured points are described in a robot coordinate system.

B. Determination of desired posture

Let the measured points V assume the trimmed points $\{v_1, ..., v_m\}(m \leqq n)$ and generate the least-squares plane based on the new measured points. The parameters a, b, and c of the least-squares plane $z = ax + by + c$ are determined by the following equations (an overbar indicates an average on m measured points):

$$a = \frac{\alpha_{z,x}\alpha_{y,y} - \alpha_{x,y}\alpha_{y,z}}{\alpha_{x,x}\alpha_{y,y} - \alpha_{x,y}\alpha_{x,y}} \quad (2)$$

$$b = \frac{\alpha_{y,z}\alpha_{x,x} - \alpha_{x,y}\alpha_{z,x}}{\alpha_{x,x}\alpha_{y,y} - \alpha_{x,y}\alpha_{x,y}} \quad (3)$$

$$c = \overline{z_v} - \overline{x_v}a - \overline{y_v}b \quad (4)$$

$$\alpha_{x,y} = \overline{x_v \cdot y_v} - \overline{x_v} \cdot \overline{y_v} \quad (5)$$

$$\alpha_{y,z} = \overline{y_v \cdot z_v} - \overline{y_v} \cdot \overline{z_v} \quad (6)$$

$$\alpha_{z,x} = \overline{z_v \cdot x_v} - \overline{z_v} \cdot \overline{x_v} \quad (7)$$

$$\alpha_{x,x} = \overline{x_v \cdot x_v} - \overline{x_v} \cdot \overline{x_v} \quad (8)$$

$$\alpha_{y,y} = \overline{y_v \cdot y_v} - \overline{y_v} \cdot \overline{y_v} \quad (9)$$

Then, a translation to the coordinate system if the robot body is parallel to the least-squares plane of the ground surface and it makes contacts with the ground is described by the following equation in quaternion algebra:

$$\begin{bmatrix} 0 \\ x_{v'_i} \\ y_{v'_i} \\ z_{v'_i} \end{bmatrix} = q' \times \begin{bmatrix} 0 \\ x_{v_i} \\ y_{v_i} \\ z_{v_i} \end{bmatrix} \times q'^{-1} - \begin{bmatrix} 0 \\ 0 \\ 0 \\ \max(z_{v'}) \end{bmatrix} \quad (10)$$

$$q' = \begin{bmatrix} \cos\frac{\theta_{rot}}{2} \\ b\sin\frac{\theta_{rot}}{2} \\ -a\sin\frac{\theta_{rot}}{2} \\ 0 \end{bmatrix} \quad (11)$$

$$\theta_{rot} = \cos^{-1}\frac{1}{\sqrt{a^2+b^2+1}} \quad (12)$$

C. Determination of desired positions of flippers

Let $V' = \{v'_1, ..., v'_m\}$ be the target measured points converted coordinates to (10). To calculate the desired flipper positions that realize the desired posture, we consider that the body is in the desired posture and that the flipper makes contact with a measured point on the coordinate system (10) for each flipper and each measured point. The contact angle for each desired flipper position is determined with one measured point that maximizes the contact angle.

Kenaf's flipper has a round toe. We can distinguish whether or not every measured point makes contact with its straight or round section by the distance d between its support point and the measured point. The threshold $d_{threshold}$ for d equals the distance from the support point to the boundary point between the straight and round sections. $d_{threshold}$ is given by the following equation:

$$d_{threshold} = \sqrt{r^2 + L^2 - (R-r)^2} \quad (13)$$

where r is the radius of a support-point-centered round section; R, the radius of the round toe section; and L, the distance between the centers of these round sections.

First, we consider the case in which contact is made with the straight section ($d \leqq d_{threshold}$). Fig. 3 shows the orientation of the flipper in this case. From Fig. 3, a contact angle of the flipper $\theta_{contact}$ with a measured point on the straight section is described by following equation:

$$\begin{aligned} \theta_{contact} &= \theta_1 + \theta_2 \\ &= \tan^{-1}\frac{z_{v'}}{x_{v'} - x} \\ &\quad + \sin^{-1}\frac{r}{\sqrt{(x_{v'} - x)^2 + {z_{v'}}^2}} \end{aligned} \quad (14)$$

Second, we consider a case in which contact is made with the round section ($d_{threshold} < d$). Fig. 4 shows the orientation of the flipper in this case. From Fig. 4, the following relationship about θ_1 is observed because the distance between the center of the round toe section and the measured point equals R.

$$R^2 = (x_{v'} - L\cos\theta_1)^2 + (z_{v'} - L\sin\theta_1)^2 \quad (15)$$

$$= d^2 + L^2 - 2L\left[x_{v'}\sin\theta_1 + z_{v'}\cos\theta_1\right] \quad (16)$$

$$= d^2 + L^2 - 2Ld\sin\left(\theta_1 + \tan^{-1}\frac{x_{v'}}{z_{v'}}\right) \quad (17)$$

$$\therefore \theta_1 = \sin^{-1}\frac{d^2 + L^2 - R^2}{2Ld} - \tan^{-1}\frac{x_{v'}}{z_{v'}} \quad (18)$$

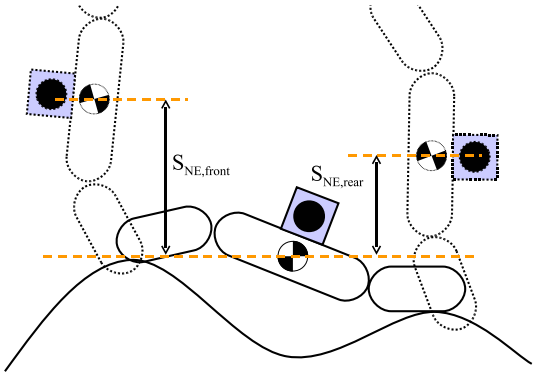

Fig. 5. NESM of Kenaf

Therefore, the contact angle of the flipper $\theta_{contact}$ with a measured point on the round section is given by the following equation:

$$\begin{aligned}\theta_{contact} &= \theta_1 - \theta_2 \\ &= \sin^{-1}\frac{d^2+L^2-R^2}{2Ld} - \tan^{-1}\frac{x_{v'}}{z_{v'}} \\ &\quad - \sin^{-1}\frac{R-r}{L} \end{aligned} \tag{19}$$

We apply above calculations about contact angles to the measured points $V' = \{v'_1, ..., v'_m\}$, and we adopt the maximum contact angle $\theta_{contact}$ observed for the cases of contact with the straight and round sections as the desired flipper position.

$$\theta_{ref} = \max(\theta_{contact}) \tag{20}$$

A measured point that maximizes $\theta_{contact}$ is assumed to be a contact point with the flipper, and it is used in evaluating the stability of a desired pose in Sec. III-D.

D. Stability evaluation of desired pose

1) Stability criterion of pose of robot: In the proposed controller, we adopt the normalized energy stability margin (NESM) [7][8] proposed by Hirose et al. as a stability criterion for the desired pose. The stability of a desired pose is evaluated by the NESM, and the pose is redefined if the stability is not sufficient. The NESM is a criterion that is used to evaluate the stability of a robot based on the vertical distance between the initial position of the center of gravity and its highest position during tumbling (Fig. 5). Although it is mainly used for walking robots, its evaluation only requires the positions of contact points with the ground surface and the center of gravity of the robot. In other words, there is no conceptual difference when applying this criterion to the case of tracked vehicles having flippers.

In the case of Kenaf, four contact points (front-right, front-left, rear-right, and rear-left) can be determined by the procedure described in Sec. III-C. In addition, four axes of tumbling that pass through the front, rear, right, and left contact points can be assumed. The stability of Kenaf is determined by the minimum value of the NESM about these four axes.

In a real environment, robots may not tumble about a static axis because of a shift in the contact points. However, simulating such a situation requires a complex analysis that may require information about an area that cannot be detected by the laser range sensors. Therefore, for the sake of simplicity, we achieve a trade-off between the accuracy and convenience of evaluation and assume tumbling about a static axis in the proposed controller.

2) Calculation of NESM: Let g_1 and g_2 be contact points and c be the center of gravity of Kenaf in the robot coordinate system. A conversion to a coordinate system having the z-axis as the vertical is described by the following equation including the posture quaternion of Kenaf q:

$$g'_1 = q \times g_1 \times q^{-1} \tag{21}$$
$$g'_2 = q \times g_2 \times q^{-1} \tag{22}$$
$$c' = q \times c \times q^{-1} \tag{23}$$

For descriptive purposes, we assume $z_{g'_1} < z_{g'_2}$. Then, let u_g and u_c be vectors that are generated by g'_1, g'_2, and c', respectively, and p_{foot} be the foot of a perpendicular from c' to u_g. These are given by the following equations:

$$u_g = g'_2 - g'_1 \tag{24}$$
$$u_c = c' - g'_1 \tag{25}$$
$$p_{foot} = g'_1 + \frac{|u_g \cdot u_c|}{|u_g|}\frac{u_g}{|u_g|} \tag{26}$$

Then, the highest position $p_{highest}$ of the center of gravity when tumbling around u_g is described by the following equations:

$$p_{highest} = p_{foot} + |p_{foot} - c'|\frac{u_{highest}}{|u_{top}|} \tag{27}$$
$$u_{highest} = [0,0,1]^t - \frac{|[0,0,1]^t \cdot u_g|}{|u_g|}\frac{u_g}{|u_g|} \tag{28}$$

The NESM S_{NE} about the contact points g_1 and g_2 is given as

$$S_{NE} = z_{p_{highest}} - z_{c'} \tag{29}$$

E. Redefinition of desired pose

When the NESM of Kenaf is less than a predetermined threshold, we repeat the following routine until a desired, stable pose is realized.

1a. When the NESM about the front or rear is adopted, reduce the pitch angle of the desired posture close to zero.

1b. When the NESM about the right or left is adopted, reduce the roll angle of the desired posture close to zero.

2. Redefine the desired flipper positions by recalculating them to realize the redefined desired posture.

3. Evaluate the NESM about the redefined posture and flipper positions.

F. Position control of flippers

Finally, position control of the flippers is performed. The desired flipper position is realized using the abovementioned procedures based on the strategy described in Sec. II.

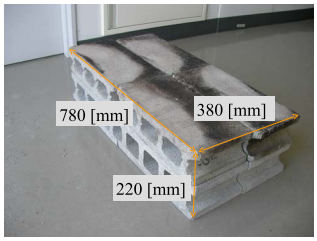

Fig. 6. A step comprising concrete blocks

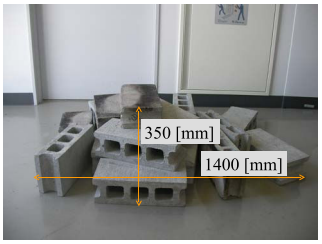

Fig. 7. Complex terrain comprising randomly positioned concrete blocks

The Kenaf's flippers are controled by a microprocessor on built-in motor driver. The desired flipper positions is sent to the microprocessor as a reference of the position control using the conventional PID-controller.

IV. Experiments

A. Overview

We implemented the proposed controller in Kenaf and performed experiments on several rough terrains comprising concrete blocks. The following two experimental results are typical ones for validating our proposed method.

We set up two experimental fields—a simple step (Fig. 6) and a pile of concrete blocks (Fig. 7). The posture of Kenaf while it traverses the experimental fields is measured using its built-in gyroscopes.

In every traversal, Kenaf was teleoperated and it moved with a velocity of approximately 5 to 10 $[cm/s]$. In the following sections, we compare traversals in which the proposed controller is used to control the flippers with ones in which routine or static motion of the flippers is used. In all trials, we assumed the estimated time delay Δt between scanning the terrain and swinging the flippers to be 0.3 $[s]$ and the threshold of the NESM to be half of that on level ground.

B. Experiment on a simple step

First, an experiment on a simple step comprising 8 concrete blocks (Fig. 6) was performed. We constructed a comparative routine motion of the flippers that duplicates flipper motions by an expert operator as follows. We assumed the angle of the flipper to be $0°$ when its straight section was in contact with flat ground, and the direction of the flipper lifting up its toe from $0°$ was considered to be positive.

1) From the beginning of the traversal until the main track makes contact with the top surface of the step: all positions of $45°$
2) Until the center of gravity of Kenaf is above the top surface of the step: all positions of $-45°$
3) While the center of gravity of Kenaf is above the top surface of the step: all positions of $0°$
4) Until the front flippers make contact with the floor surface: all positions of $-45°$
5) Until the traversal is complete: all positions of $45°$

What aspect Kenaf was on was determined by our observations and we controlled the flipper positions. In addition, to confirm the validity of the stability evaluation and desired pose redefinition referred to in Sec. III, a traversal using the proposed controller without these procedures was also performed.

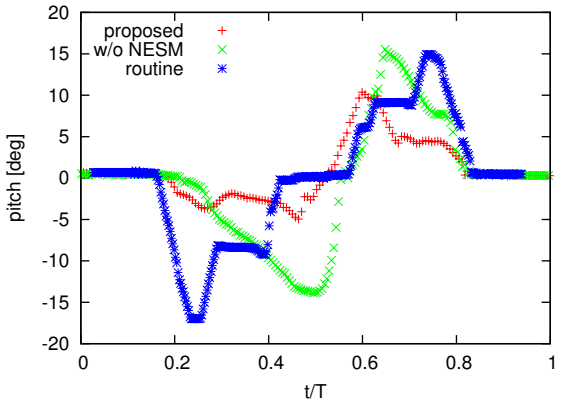

Fig. 8. Change in pitch angles while traversing the step

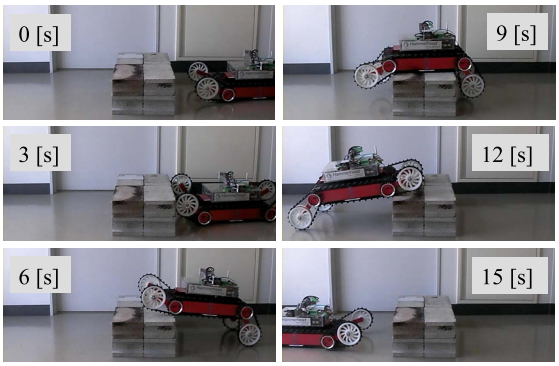

Fig. 9. Snapshots while traversing the step

Fig. 8 shows the change in the pitch angles of Kenaf during the traversal and Fig. 9 shows snapshots of the traversal when using the proposed controller. For the purpose of comparison, the horizontal axis in Fig. 8 indicates ratios obtained by dividing the elapsed times by the total time required to traverse a step.

The graph and snapshots show that the proposed controller kept the pitch angle negative (nose-up posture) and positive (nose-down posture) when climbing up and down the step, respectively, even without stability evaluation. This behavior is similar to the traversal with the expert-simulated routine motion. This result indicates that the proposed method can generate flipper motions that replicate those of an expert, as described in Sec. III.

A difference between the control methods can be observed from Fig. 8. The proposed controller without stability evaluation and the routine motions generates pitch angles ranging from $-20°$ to $20°$. However, the proposed controller limited the pitch angles to between $-10°$ and $10°$. This difference is attributed to the redefinition of the desired pose based on an evaluation of the NESM. This result may not indicate whether the proposed controller is optimal because of the trade-off between the height of a step and the maximum value of the pitch angle on climbing it. However, from the viewpoint of the extent to which control of the flipper motion

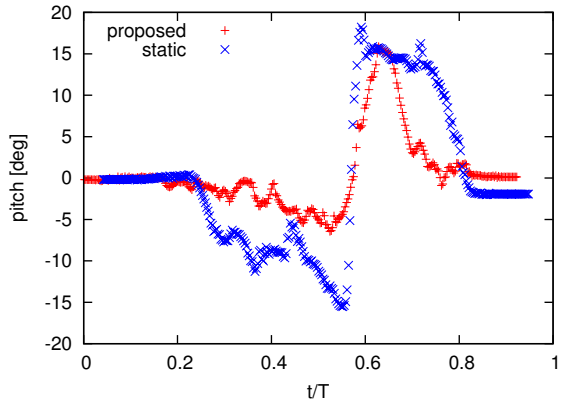

Fig. 10. Change in pitch angles while traversing the complex field

reduces the risk of the robot's rollover, we consider that the proposed controller generated the most optimal motions in this environment.

C. Experiment on a pile of concrete blocks

Second, an experiment on a complex field comprising 16 concrete blocks (Fig. 7) was performed. We adopted a comparative case with static flipper angles of $45°$.

Fig. 10 shows the change in the pitch angles of Kenaf during the traversal and Fig. 11 shows snapshots of the traversal when using the proposed controller.

Although a rapid motion similar to freefall occurred around the top of the field with static flipper positions, it did not occur when using the proposed controller (Fig. 12). This is also confirmed from the graph shown in Fig. 10. In the middle of the traversal, a rapid swing of the pitch angles with a maximum angular velocity of 61.8 $[°/s]$ appears when using static flipper positions. On the other hand, the transition of the pitch angles when using the proposed controllers is much smoother in comparison, and the maximum angular velocity was only 28.1 $[°/s]$. This result may be attributable to the fact that the proposed controller can generate flipper motions that are likely to not trigger rapid motions of the body because the generated motions are based on smooth movements over the ground surfaces.

V. Conclusions

In this study, we proposed an autonomous controller for active flippers that realizes stable motion of a robot body on rough terrain. The proposed controller maintains the posture of the robot body according to the average attitude above the ground surface. In addition, it evaluates the stability of the desired pose of the robot using the normalized energy stability margin to avoid the rollover of the robot. We performed experiments on rough terrain and confirmed that the proposed controller can realize semi-autonomous operation that is as smooth as teleoperation by an expert operator.

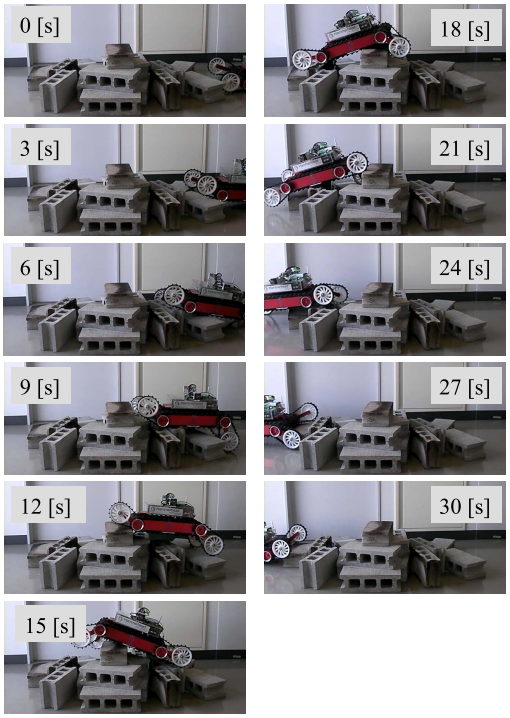

Fig. 11. Snapshots while traversing the complex field

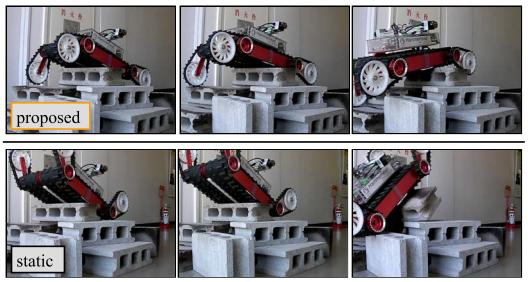

Fig. 12. Snapshots around the top of the complex field

References

[1] S.Tadokoro, F.Matsuno and A.Jacoff, "Special Issues on Rescue Robotics", Advanced Robotics Vol.19 No.3, No.8, 2004

[2] A. Jacoff, E. Messina, B.A. Weiss, S. Tadokoro and Y. Nakagawa, "Test Arenas and Performance Metrics for Urban Search and Rescue Robots", *the IEEE/RSJ International Conference on Intelligent Robots and Systems*, Las Vegas, NV, 2003, pp. 3396-3403

[3] K. Nagatani, A. Yamasaki, K. Yoshida, T. Yoshida and E. Koyanagi, "Improvement of the Operability of a Tracked Vehicle on Uneven Terrain using Autonomous Control of Active Flippers", *the IEEE/RSJ International Conference on Intelligent Robots and Systems*, Nice, France, 2008, pp. 2717-2718

[4] K. Nagatani, N. Tokunaga, Y. Okada and K. Yoshida, "Continuous Acquisition of Three-dimensional Environment Information for Tracked Vehicles on Uneven Terrain", *the IEEE International Workshop on Safety, Security, and Rescue Robotics*, Sendai, Japan, 2008, pp. 25-30

[5] M. Kim, W. Lee and S. Kang, "Robhazdt3: Teleoperated Mobile Platform with Passively Adaptive Double-track for Hazardous Environment Applications", *the IEEE/RSJ International Conference on Intelligent Robots and Systems*, Sendai, Japan, 2004, pp. 33-38

[6] K. Ohno, S. Morimura, S. Tadokoro, E. Koyanagi and T. Yoshida, "Semi-autonomous Control System of Rescue Crawler Robot Having Flippers for Getting Over Unknown-steps", *the IEEE/RSJ International Conference on Intelligent Robots and Systems*, San Diego, CA, 2007, pp. 3012-3018

[7] S. Hirose, H. Tsukagoshi and K. Yoneda, "Normalized Energy Stability Margin: Generalized Stability Criterion for Walking Vehicles", *the International Conference on Climbing and Walking Robots*, Brussels, Belgium, 1998, pp. 71-76

[8] S. Hirose, H. Tsukagoshi and K. Yoneda, "Normalized Energy Stability Margin and its Contour of Walking Vehicles on Rough Terrain", *the IEEE International Conference on Robotics and Automation*, Seoul, Korea, 2001, pp. 181-186